circPTP4A2-miR-330-5p-PDK2 Signaling Facilitates In Vivo Survival of HuMSCs on SF-SIS Scaffolds and Improves The Repair of Damaged Endometrium

Yuanyuan Zheng
The First Affiliated Hospital of ZhengzhouUniversity
Linhao Li
BeiHang University School of Biological Science and Medical Engineering
Xuewei Bi
Beihang University
Ruyue Xue (fccxuery@zzu.edu.cn)
Zhenzhou University https://orcid.org/0000-0001-9028-7794

Research

Keywords: Intrauterine adhesions, Human umbilical cord MSCs (HuMSC), Silk fibroin surface modified small-intestinal submucosa (SF-SIS), CircPTP4A2, Mitochondrial metabolism

Posted Date: September 30th, 2021

DOI: https://doi.org/10.21203/rs.3.rs-895708/v1

Abstract

Background

Human umbilical cord MSCs (HuMSC)-based therapy has shown promising results in the treatment of intrauterine adhesions (IUA). In this study, our aim was to construct a HuMSC-seeded silk fibroin small-intestinal submucosa (SF-SIS) scaffold and evaluate the impact of repairing the damaged endometrium in an IUA mouse model.

Methods

To identify the functional effect of HuMSCs-silk cellulose (SF)- small-intestinal submucosa (SIS) scaffolds on the repair of damaged endometrium, a mouse IUA model was established in this study. The uterine morphology and fibrosis were evaluated by hematoxylin - eosin (H&E) staining and Masson staining. CircRNA sequencing, real-time PCR and RNA fluorescence in situ hybridization were used to screen and verify the potential circRNAs that involved in the repair of damaged endometrium by HuMSCs. Real time integrated cellular oxygen consumption rate (OCR) was measured using the Seahorse XF24 Extracellular Flux Analyser. The potential down-stream miRNAs and proteins of circRNAs were analyzed dual-luciferase report and Western Blot.

Results

We found that HuMSCs-SF-SIS not only increased the number of glands, but also reduced the ulcer area in the IUA model. Furthermore, we demonstrated that circPTP4A2 was elevated in the HuMSCs seeded on the SF-SIS scaffolds and stabilized the mitochondrial metabolism through miR-330-5p-PDK2 signaling, which contributes to endometrial repair progression.

Conclusion

In this study, we demonstrated that circPTP4A2 was elevated in the HuMSCs seeded on the SF-SIS scaffolds and stabilized the mitochondrial metabolism through miR-330-5p-PDK2 signaling, which contributes to endometrial repair progression. These findings demonstrate that HuMSC-seeded SF-SIS scaffolds are an encouraging method for the treatment of IUA.

1. Introduction

Embryo implantation failure caused by female endometrial damage is the main factor affecting the success rate of assisted reproduction. Cells in the functional layer of the endometrium in a normal cycle are apoptotic and shed, and release signals to activate endometrial stem cells (ESCs), promoting angiogenesis and tissue repair. However, after the damage, the endometrium is deficient in blood vessels

and has few glands leading to thinning of the uterine lining (atrophy)[1, 2]. Intrauterine adhesions (IUA), also called Asherman's syndrome, is a common uterine disease caused by damage to the basal lining of the endometrium caused by mechanical injury or infection, resulting in endometrial fibrosis, uterine obstruction, menstrual abnormalities, infertility and pregnancy [3, 4]. Presently, hysteroscopic adhesiolysis is performed clinically, and anti-adhesion drugs and IUD are administered simultaneously [5]. Several therapeutic agents have been used to improve endometrial regrowth [6]. However, due to the loss and functional destruction of endometrial basal stem cells, the therapeutic effect is not ideal, and a normally functional endometrial environment cannot be provided.

Mesenchymal stem cells can differentiate into endometrial epithelial and mesenchymal cells after induction, suggesting that mesenchymal stem cells have biological functions similar to those of endometrial basement ESCs and may be involved in the repair of the endometrial structure and improve its function [7]. However, multiple challenges persist in the treatment of endometrial damage by exogenous mesenchymal stem cells, such as differences in the cell carrier and the intrauterine environment [8]. Generally, human umbilical cord MSCs (HuMSCs) were superior to bone marrow MSCs (BM-MSCs) in terms of cell content and proliferative capacity, and have lower immunogenicity than BM-MSCs [9, 10]. In addition, (HuMSCs) are convenient to obtain materials and are free from ethical controversies, and other advantages have attracted increasing attention [11]. Studies using in vivo HuMSC transplantation experiments to observe endometrial reconstruction, two months after the detection of transplantation, showed a thickening of the damaged endometrial tissue, a reduction in the area affected by fibrosis, and a similar repair period. It is speculated that HuMSCs secreted by paracrine factors have anti-inflammatory effects, facilitate the repair of the endometrium, and maintain cell function and angiogenesis of the microenvironment [12]. However, the molecular mechanism underlying the effect of HuMSCs on the repair and regeneration of the endometrium remains unclear.

Recently, a significant focus has been expressed on the application of tissue-engineered artificial reconstruction materials for tissue repair and regeneration. Small-intestinal submucosa (SIS) is a cell-free, allogeneic, and collagen-matrix material with good histocompatibility and biomechanical properties and no immunogenicity and toxicity [13]. It is a natural biodegradable biological material [14–16]. The submucosa of the small intestine is mainly composed of type I collagen isotype, and is rich in fibronectin and growth factors, among which aplasia collagen and fibronectin can specifically bind to the cell membrane and activate the cell conduction pathway to facilitate cell adhesion[17]. As a tissue-engineered material, SIS has been widely used in the research of cartilage, tendon, bladder, cardiovascular regeneration, and other fields, however a few studies have been reported on the repair of injuries of the endometrium and the molecular mechanism [18, 19]. Silk cellulose (SF) has the three advantages of good mechanical properties, controllable biodegradation and excellent biocompatibility, and has been widely used in the field of biomedicine [20, 21]. The SIS membrane is a material coated with SF layers, which can adjust the diffusion rate of drugs or biomolecules and improve the mechanical and structural stability of its properties.

In this study, we constructed HuMSC-seeded SIS scaffolds and evaluated the impact of the repair of damaged endometrium in an IUA mouse model. Moreover, We also studied the potential mechanism of HuMSCs in repairing the endometrium.

2. Materials And Method

2.1 Preparation and characterization of SF-SIS scaffolds

The SF-SIS scaffolds used in this study was kindly donated from Dr. Li (The Key Laboratory for Biomechanics and Mechanobiology of Ministry of Education, School of Biological Science and Medical Engineering, Beihang University, Beijing, China). The SF-SIS scaffolds were prepared and characterized as previously described [20].

2.2 Characterization and culture of HuMSCs

HuMSCs is purchased from Promocell (Miaotong (Shanghai) Biological Science & Technology Co., Ltd. Shanghai, China). Frozen HuMSCs between P2 and P10 were freshly inoculated in 100 mm culture dishes (1×10^6 cells per dish) supplemented with 10% (v/v) fetal bovine serum (FBS, Gibco, USA), penicillin (100 U/ml, Gibco) and Streptomyces (100 mg/ml, Gibco). Briefly, the phenotype of HuMSCs was identified by FACS specificity (CD34, CD45, CD29, CD90, CD105 and HLA-DR). The osteogenic and adipogenic abilities of mesenchymal stem cells were determined by the Cyagen Osteogenic stimulation kit (Cyage, Guangzhou, China) and the Cyagen Adipogenic Differentiation Kit (Cyage, Guangzhou, China).

2.3 Osteogenic and adipogenic differentiation of HuMSCs

According to the manufacturer's instructions (RASMX-90021 and RASMX-90031, Cyagen, Guangzhou, China), the ability of cells to differentiate into osteoblasts or adipocytes was characterized using commercial osteogenic and adipogenic induction kits. Osteoblasts were stained with Alizarin Red S and adipocytes with oil red O.

2.4 Animal IUA model

All animal procedures are approved by the the first affiliated hospital of Zhengzhou University, Institutional Animal Care and Use Committee and are carried out in accordance with the National Research Council Laboratory Animal Care and Use Guidelines. 6-week-old BALB /c mice were obtained from Shanghai SLAC Animal Center and allowed to acclimatize to the new environment for a week. To establish an IUA model, the uterus was mechanically damaged during pregnancy. Mice were anesthetized by intraperitoneal injection of sodium pentobarbital. The uterus is excised at the midline below the abdomen. Insert a size 7 needle into the left and right uterine junction and cut it carefully back and forth until the uterine congestion is visible to the naked eye. Then, the abdominal cavity was closed. The operation was performed under aseptic conditions. The control group did not undergo surgery.

2.5 Histological analysis

Uterine specimens were collected 8 days after surgery. The sample was fixed with 4% paraformaldehyde, dehydrated, removed with xylene, and finally embedding with paraffin. The embedded tissue sections were 5-μm thick. The uterine morphology and structure were evaluated by hematoxylin - eosin (H&E) staining. Masson staining was performed to evaluate the fibrosis according to manufacturer's instructions (Yeasen, Shanghai, China). Fibrosis areas (light blue) were evaluated using ImageJ software (MD, USA).

2.6 circRNA sequencing

Total RNAs were extracted with Trizol (Invitrogen, Carlsbad, CA, USA). Sequencing libraries were generated and sequenced by Sango Bio Technology (Shanghai, China). A total amount of 5 μg RNA per sample was used. The libraries were subjected to paired-end sequencing with pair end 150 bp reading length on an Illumina HiSeq sequencer (Illumina, San Diego, CA, USA).

2.7 Real-time PCR

Total RNA was extracted with Trizol reagent (TAKARA), and 500 ng total RNA was transcribed into cDNA using PrimeScript RT Master Mix (TAKARA, Dalian, China). Subsequently, SYBR Premix Ex Taq II Kit (TAKARA) was used to detect the expression of circRNAs and mRNA by RT-qPCR, which was normalized to endogenous control GAPDH expression. Folding changes were calculated using $2^{-\Delta\Delta CT}$ method.

2.8 RNA fluorescence in situ hybridization

RNA fluorescence in situ hybridization was performed using a fluorescence in situ hybridization kit (RiboBio, Guangzhou, China) in accordance with the manufacturer's guidelines. Cy3-labeled circPTP4A2 probe (RiboBio, Guangzhou, China) was detected with fluorescence in situ hybridization kit and then observed with LSM800 confocal microscopy (Zeiss, Germany).

2.9 Measurement of mitochondrial metabolism

ATP content and synthase activity was performed using the quantification kits (Sango Biotech, Shanghai, China) in accordance with the manufacturer's guidelines. Real time integrated cellular oxygen consumption rate (OCR) was measured using the Seahorse XF24 Extracellular Flux Analyser (Seahorse Bioscience, North Billerica, MA, USA) as previous described. In brief, HuMSCs cells were treated with 10 μg/mL curcumin for 12 h and 10^4 cells were plated into the seahorse customized cell plates. After the probes were calibrated, the OCR was detected with sequential injection of the following compounds which regulate mitochondrial respiration: oligomycin (ATP synthase inhibitor; 1 μM), FCCP (uncoupler; 1 μM), rotenone (complex I inhibitor; 1 μM), and antimycin A (complex III inhibitor; 1 μM).

2.10 Dual-luciferase reporter assays

The 293T cells were incubated in 24-well plates with 2×10^4 cells per well. These cells were then transfected with psiCheck2-circPTP4A2-WT or psiCheck2-circPTP4A2-Mut, miR-330-5p mimics, or miR-NC. After 48 h, the cells were lysed with a passive lysis buffer (Promega, Madison, WI, USA) and the dual

luciferase reporting assay (Promega) was used to calculate the relative luciferase activity by normalized firefly luminescence to Renilla luminescence.

2.11 Western blotting

The HuMSCs were lysed with RIPA lysis buffer. The same amount of protein was then broken down by SDS-PAGE analysis and electrically transferred to PVDF membranes (Milliore, Schwalbach, Germany), which were then sealed with 5% skimmed milk powder and incubated overnight with primary antibody at 4°C. The primary antibodies used were anti-PDK2 (Cell Signaling Technology) and anti-GAPDH (Kanchen Biotech). The membrane was then incubated with HRB-conjugated secondary antibodies at room temperature for 1 h, and the imprinting was observed using an enhanced chemiluminescence kit (Pierce, Waltham, MA, USA).

2.12 Statistical Analysis

Data were expressed as the Means ± SEM. For two groups, 2-tailed t-test (unpaired) was used for comparisons. For multiple comparisons, ANOVA followed by the post hoc Bonferroni test was taken with GraphPad Prism® version 9.0 software (GraphPad Software, Inc., La Jolla, CA, USA).

3. Results

3.1 Culture and characterization of HuMSCs

BMSCs are adsorbed on plastic discs. The typical morphology of HuMSCs is similar to that of spindle-shaped fibroblasts, which grow in a tightly packed vortex pattern, is shown in Fig. 1A. The HuMSCs were successfully differentiated into osteoblasts and adipocytes in vitro (Fig. 1A), this indicates that this cell population was a pluripotent mesenchymal stromal cell. Furthermore, FACS results showed that most cells were negative for hematopoietic markers after 7 days in culture for CD34+ (5.12%), CD45+ (2.05%), HLA-DR (0.61%) and highly positive for CD29 (61.9%), CD90 (94.9%) and CD105 (94.9)%.expression (Fig. 1B).

3.2 HuMSCs-SF-SIS reduces fibrotic area and increases the number of glands in the IUA model

To identify the functional effect of HuMSCs-SF-SIS scaffolds on the repair of damaged endometrium, a mouse IUA model was established.The HuMSCs-SF-SIS scaffolds were transplanted after the damage to the endometrium was reduced. After 4 weeks, uterine tissue was collected up for modeling. According to the HE staining results, the shape of the uterine cavity in the pseudopod group was irregular. Columnar epithelial cells cover the uterus and gland cavities. Epithelial cell structure was complete, stromal glands were abundant, and oval. Connective tissue fragments were found in the uterine cavity in the IUA model group, the number of glandular blood vessels were significantly reduced, and the connective tissue was congested one week after the damage. The number of endometrial glands in the HuMSCs-SF-SIS

transplanted group increased, and the lumen of neonates was not completely covered by the monolayer columnar epithelium (Fig. 2A,$P < 0.05$). According to the results of statistical analysis, for the number of endometrial glands, the model group and HuMSCs-SF-SIS transplantation group were lower than the sham-operated group (Fig. 2B, $P < 0.05$), and the model group was significantly lower than the sham-operated group ($P < 0.05$). Differently, the group of HuMSCs-SF-SIS transplantation group was significantly higher than the IUA model group (Fig. 2B, $P < 0.05$). Endometrial adhesions are characterized by fibrosis. In the study, we used Masson staining (Fig. 2C) to assess the degree of fibrosis. A significant increase in the area of endometrial fibrosis was observed in IUA model mice compared with the sham group (Fig. 2D,$P < 0.05$), but HuMSCs-SF-SIS transplantation resulted in a significant decrease in fibrosis (Fig. 2D, $P < 0.05$). In conclusion, transplantation of HuMSCs-SF-SIS not only increased the number of endometrial glands, but also repaired the injured endometrium.

3.3 The expression level of circPTP4A2 was significantly elevated in the HuMSCs cultured on the SF-SIS scaffolds

To explore whether circRNA is involved in endometrial repair, we first performed RNA-seq analysis of total RNA from ribosomal RNA of normal HuMSCs and HuMSCs cultured on SF-SIS scaffolds (Fig. 3A). A total of 54 circRNAs were significantly downregulated, and 27 circRNAs were upregulated in HuMSCs cultured on the SF-SIS scaffolds (filtered by FC(fold change) > 2 and $P < 0.05$). Variability expression of circRNAs was directly displayed by volcano clustering analysis. (Fig. 3B). We then chose several significantly upregulated circRNAs (circUXSI, circPTP4A2, circCNTRL, circEPSTII, circSFMBT2, circZNF680, and circEMB) to verify their existence via real-time PCR (Fig. 3C). We concluded that circPTP4A2 was upregulated in HuMSCs cultured on the SF-SIS scaffolds (Fig. 3C). In a follow-up study, we found resistance between circPTP4A2 and RNase R and also confirmed that PTP4A2 mRNA showed a significant reduction after RNase R treatment (Fig. 3D). Moreover,(sub-fractional real-time PCR (Fig. 3E) and fluorescence in situ hybridization (FISH) assays (Fig. 3F) data indicated that circPTP4A2 was mainly present in the cytoplasm.

3.4 CircPTP4A2 facilitates the mitochondrial metabolism of HuMSCs under hypoxia condition

Mitochondria are essential in the cellular biochemistry of most eukaryotic cells, producing nearly 95% of cellular ATP through oxidative phosphorylation of mitochondria, thereby controlling cell death or survival under hypoxic conditions, such as the transplanted SF-SIS scaffolds. Considering the critical role of mitochondrial metabolism, we tested whether circPTP4A2 facilitates the biological functions of HuMSCs via the regulation of mitochondrial metabolism. For the purpose of hypothesis testing, we first determined the effects of circPTP4A2 on ATP content (Fig. 4A) and ATP synthase activity (Fig. 4B).We found that the ATP content and ATP synthase activity were dramatically decreased in hypoxic HuMSCs, but significantly increased with the overexpression of circPTP4A2. Using the seahorse XF24 extracellular flux analyzer, we also analyzed the cell oxygen consumption rate (OCR) (Fig. 4C), indicating reduced OXPHOS in HuMSCs cells. We then assessed the mitochondrial functions, in particular, basal respiration (Fig. 4D), maximal

respiration (Fig. 4F), ATP production (Fig. 4E), spin respiratory capacity (Fig. 4G), proton leak (Fig. 4H), and non-mitochondrial respiration (Fig. 4I). Hypoxia treatment dramatically impaired the OCR value of basal respiration, spare respiratory capacity, maximal respiration, and ATP production in HuMSCs. In contrast, overexpression of circPTP4A2 significantly attenuated the inhibitory effect of hypoxia on ATP content, ATP synthase activity, and cell oxygen consumption rate (OCR). These data indicate that circPTP4A2 could facilitate the mitochondrial metabolism of HuMSCs under hypoxic conditions.

3.5 CircPTP4A2 is targeted by miR-330-5p in HuMSCs cells

To explore whether circPTP4A2 can function as “miRNA sponge” in HuMSCs cells, we selected several potential miRNAs (miR-326, miR-487a, miR-335, miR-532-3p, miR-421, miR-502-5p, miR-330-5p, miR-1290 and miR-1305) through Starbase 2.0 database. After circPTP4A2 knockout, we found an increased level of miR-330-5p (Fig. 5A) in HuMSCs cells. Enrichment of miR-330-5p with circPTP4A2 was derived from the Ago2 co-immunoprecipitation assay (Fig. 5B) and miR-330-5p RNA pull-down assay (Fig. 5C). To further verify the miR-330-5p target circPTP4A2, we added a luciferase reporter gene test. The results showed that miR-330-5p mimics significantly reduced the luciferase activity of HuMSCs transfected with wild-type circPTP4A2. But the miR-330-5p mimic failed to reduce the luciferase activity of the mutant circPTP4A2 transfected HuMSCs cells (Fig. 5D). These results suggest that circPTP4A2 is targeted by miR-330-5p in HuMSCs.

3.6 MiR – 330- 5p over-expression impaired the circPTP4A2 enhanced mitochondrial metabolism in hypoxia - treated HuMSCs.

To identify whether miR – 330–5p is critical to circPTP4A2 enhanced mitochondrial metabolism in hypoxia – treated HuMSCs. We transfected the miR – 330–5p mi mic in hypoxia - treated HuMSCs with or without circPTP4A2 overexpression. The miR – 330–5p mimic dramatically reduced ATP content (Fig. 6A) and ATP synthase activity (Fig. 6B). Moreover, miR-330-5p mimics the Reduced basal respiration, spare respiratory capacity, ATP produ ction, and maximal respiration in HuMSCs cells (Fig. 6C). Notably, circPTP4A2 overexpression failed to increase basal respiration (Fig. 6D), ATP production (Fig. 6E), maximal respiration (Fig. 6F) ,and spare respiratory capacity(Fig. 6G) in HuMSC cells transfected with miR-330-5p mimic. Through the above results, it is shown that miR-330-5p overexpression impaired circPTP4A2 enhanced mitochondrial metabolism in hypoxia - treated HuMSCs.

3.7 MiR – 330–5p inhibits PDK2 expression through the 3' UTR target region

To further explore the underlying mechanism of the circPTP4A2/miR-330-5p axis on mitochondrial metabolism in hypoxia-treated HuMSCs, we then screened the potential targets of the miR-330-5p Target Scan and Star Base databases. Further by dual luciferase assay, we found that the 3’UTR mRNA of the mitochondrial metabolism regulator PDK2 was directly targeted by miR-330-5p (Fig. 7A-7D). In addition, PDK2 mRNA (Fig. 7B) and protein (Fig. 7C) levels were significantly reduced by miR-330-5p mimics in

mouse umbilical cord MSCs and HuMSC. Taken together, it can be concluded that miR-330-5p may regulate mitochondrial metabolism by suppressing the expression of PDK2.

3.8CircPTP4A2-miR-330-5p-PDK2 signaling is critical to HuMSCs-SF-SIS decreasing the fibrosis area and increasing the number of glands in IUA model

To confirm the critical role of circPTP4A2-miR-330-5p-PDK2 signaling in the progress of the repair of the endometrium by HuMSCs-SF-SIS in IUA model,we altered the levels of miR-330-5p and PDK2 in HuMSCs-SF-SIS in the IUA model. As shown in Fig. 8A and 8B, the number of endometrial glands in the HuMSCs-SF-SIS transplanted group was significantly impaired by miR-330-5p and PDK2 knockdown (Fig. 8A and 8B, $P < 0.05$). However, PDK2 overexpression significantly enhanced the endometrial glands in the miR-330-5p mimic-transfected HuMSCs-SF-SIS transplanted group (Fig. 8A and 8B, $P < 0.05$). Consistently, Masson staining (Fig. 8C and 8D) results showed that the area of fibrosis in the endometrium of IUA model mice was significantly increased in the miR-330-5p or PDK2 knockdown group, but PDK2 led to a remarkable reduction in fibrosis (Fig. 8D, $P < 0.05$) in miR-330-5p mimic-transfected HuMSCs-SF-SIS transplanted group. From these results it follows that circPTP4A2-miR-330-5p-PDK2 signaling is critical to HuMSCs-SF-SIS increasing the number of glands and decreasing the area of fibrosis in the IUA Model.

4. Discussion

Presently, according to reports, 2.8%-45.5% of women with IUA have impaired fertility, notably occurring after pregnancy-related dilatation and curettage in more than 90% of cases [5, 6]. Up to now, IUA has been treated mainly with both surgical and estrogenic modalities, and unfortunately, the recurrence rate is high, ranging from 20–63% [3]. Additionally, there is also a high risk for placental implantation. Therefore, it is particularly important to develop safe and feasible treatment options for patients with IUA at this time.

Mesenchymal stem cells have now been widely used for tissue repair.Gargett et al. proposed that LUA patients could reconstruct endometrial tissue with endometrial mesenchymal stem cells [1]. Nagori et al. showed that bone marrow mesenchymal stem cell transplantation was effective in promoting repair of damaged endometrium in vivo [22], a view shared by Phermthai et al. Mesenchymal stem cell transplantation has been reported to be effective in repairing endometrial defects such as infertility and endometrial hyperplasia [23, 24]. In fibrotic diseases, mesenchymal stem cells play an anti-fibrotic role, for example, pulmonary fibrosis, renal fibrosis and hepatic fibrosis can be treated with mesenchymal stem cells [25–29]. One of the typical representatives of ECM is the submucosa of the small intestine (SIS), such as skin, bone, bladder, ligaments, and abdominal wall, which has been widely used for tissue repair and clinical trials [13].After SF coating by a single-component LbL assembly, the SIS membrane exhibited good cell compatibility and are not only well resistant to rapid degradation, but also maintain structural integrity [20]. In this study, We seeded HuMSCs on the surface of the SF-SIS scaffold and were surprised to find an increase in the number of HuMSCs-seeded SF-SIS scaffold glands, as well as a reduction in the fibrotic area of the lUA model. Based on the study data, we conclude that HuMSC-seeded SF-SIS scaffolds may be used for lUA treatment.

CircRNAs are circular non-coding RNAs that are resistant to the digestive action of RNase R. CircRNAs are mainly made by selective splicing (post splicing) of information exchange between upstream splice acceptors and downstream splice donors [30, 31]. Our comparison of circRNAs with long-stranded noncoding RNAs (lncRNAs) and microRNAs (miRNAs) in mammalian cells revealed that circRNAs are better in terms of stability and conservation[32]. Meanwhile, circRNA can interfere with the expression of related genes, transcribe and interfere with RNA responses, and also act as a scaffold or template to assemble or synthesize protein complexes through circRNA sponge action [33].Recent reports have confirmed the role of several functional circRNAs in regulating tissue regeneration of MSCs. For example, the pluripotency of human embryonic stem cells (hESCs) is maintained by sponge transfection of circBIRC6 with miR-34a and miR-145 [34]. CircHIPK3 has been reported to promote a variety of cancers by absorbing multiple miRNAs through sponge uptake [35]. CircSMARCA5 inhibits glioblastoma pleomorphic cell migration but facilitates prostate cancer cell proliferation [36]. In this study, we found that circPTP4A2 is critical to HuMSCs-SF-SIS increasing the number of glands and decreasing the fibrosis area in the lUA model by targeting miR-330-5p-PDK2 signaling.

A distinctive feature of eukaryotic cells is the presence of intracellular mitochondria, which play an important role in energy metabolism and apoptosis and are essential in biological longevity[37]. In cells, mitochondria carry out complex biological reactions and are one of the most complex reactive sensing systems [38]. Recent studies have shown that balancing mitochondrial dynamics, which regulate the fate of stem cells, and morphology is crucial for maintaining tissue homeostasis[39]. Recent studies have found that mitochondrial metabolism can be significantly altered by environmental stimuli [40]. An important feature of the MSC niche is hypoxia, which has been shown over the last decade to have a key role in maintaining three aspects of stem cell survival, self-replication and pluripotency [41]. It was found that for the glycolytic pathway, transcription and synthesis of enzymes increased in hypoxic cells, but synthesis of proteins involved in mitochondrial catabolism decreased [42].The proliferation, differentiation and survival of BMSCs has been shown to be affected by culture under hypoxic pressure[43]. Cytochrome oxidase, an enzyme located at the end of the mitochondrial respiratory chain, is involved in aerobic synthesis in mammalian cells, mainly using oxygen as a substrate [27]. Under hypoxic conditions, mitochondrial size and average velocity were significantly reduced [44]. In this study, we found that circPTP4A2-miR-330-5p-PDK2 signaling is critical for the stability of mitochondrial metabolism in HuMSCs under hypoxic conditions. Collectively, we constructed HuMSC-seeded SF-SIS scaffolds and evaluated the impact of repairing damaged endometrium in an lUA mouse model. Interestingly, we performed an in-depth study of the underlying mechanisms of endometrial repair progression in HuMSCs, in which circPTP4A2 is elevated in the HuMSCs seeded on the SF-SIS scaffolds and stabilizes mitochondrial metabolism via miR-330-5p-PDK2 signaling. Furthermore, these findings demonstrated that HuMSC-seeded SF-SIS scaffolds signify future clinical applications in the treatment of lUA.

Conclusion

In this study, we demonstrated that circPTP4A2 was elevated in the HuMSCs seeded on the SF-SIS scaffolds and stabilized the mitochondrial metabolism through miR-330-5p-PDK2 signaling, which contributes to endometrial repair progression. These findings demonstrate that HuMSC-seeded SF-SIS scaffolds are an encouraging method for the treatment of IUA.

Declarations

Ethics approval and consent to participate

The study was ethically approved by the ethics committee of the First Affiliated Hospital of Zhengzhou University. The study was performed according to the international, national and institutional rules considering animal experiments and biodiversity rights. The ethics review number is 2019-KY-72.

Consent for publication

Not applicable.

Availability of data and material

The data that support the findings of this study are available from the corresponding author upon reasonable request.

Competing interests

The authors declare that they have no competing interests.

Funding

This work was supported by National Natural Science Foundation of China (31400823 to R.-Y.X, the Chinese Medical Association of Clinical Medicine Research Special Fund Project (17020600729 to R.-Y.X.),The Youth Innovation Fund of First Affiliated Hospital of Zhengzhou University (to R.-Y.X).

Authors' contributions

YYZ and RYX performed the research, analyzed data, and participated in writing the manuscript. LHL collected and analyzed the data. XWB contributed to the study performance. All authors read and approved the final manuscript. RYX conceived this study and gave final approval of this manuscript.

Acknowledgements

We thank for Jinlong Liu for the technique support and discussion.

References

1. Gargett CE, Schwab KE, Deane JA. Endometrial stem/progenitor cells: the first 10 years. Hum Reprod Update. 2016;22(2):137–63.
2. Tempest N, Maclean A, Hapangama DK. *Endometrial Stem Cell Markers: Current Concepts and Unresolved Questions*. Int J Mol Sci, 2018. 19(10).
3. Hooker AB, et al. Reproductive performance of women with and without intrauterine adhesions following recurrent dilatation and curettage for miscarriage: long-term follow-up of a randomized controlled trial. Hum Reprod. 2021;36(1):70–81.
4. Hooker AB, et al. Systematic review and meta-analysis of intrauterine adhesions after miscarriage: prevalence, risk factors and long-term reproductive outcome. Hum Reprod Update. 2014;20(2):262–78.
5. Vercellini P, et al. Endometriosis: pathogenesis and treatment. Nat Rev Endocrinol. 2014;10(5):261–75.
6. Kou L, et al. Therapeutic options and drug delivery strategies for the prevention of intrauterine adhesions. J Control Release. 2020;318:25–37.
7. Sar-Shalom Nahshon C, et al. The impact of intentional endometrial injury on reproductive outcomes: a systematic review and meta-analysis. Hum Reprod Update. 2019;25(1):95–113.
8. Chen X, et al. Transplantation of oral mucosal epithelial cells seeded on decellularized and lyophilized amniotic membrane for the regeneration of injured endometrium. Stem Cell Res Ther. 2019;10(1):107.
9. Wang L, et al. In situ repair abilities of human umbilical cord-derived mesenchymal stem cells and autocrosslinked hyaluronic acid gel complex in rhesus monkeys with intrauterine adhesion. Sci Adv. 2020;6(21):eaba6357.
10. Xin L, et al. A collagen scaffold loaded with human umbilical cord-derived mesenchymal stem cells facilitates endometrial regeneration and restores fertility. Acta Biomater. 2019;92:160–71.
11. Yang L, et al. The Regulatory Functionality of Exosomes Derived from hUMSCs in 3D Culture for Alzheimer's Disease Therapy. Small. 2020;16(3):e1906273.
12. Yao Y, et al. Exosomes derived from mesenchymal stem cells reverse EMT via TGF-beta1/Smad pathway and promote repair of damaged endometrium. Stem Cell Res Ther. 2019;10(1):225.
13. Cao G, et al. Small intestinal submucosa: superiority, limitations and solutions, and its potential to address bottlenecks in tissue repair. J Mater Chem B. 2019;7(33):5038–55.
14. Cao G, et al. Biomimetic SIS-based biocomposites with improved biodegradability, antibacterial activity and angiogenesis for abdominal wall repair. Mater Sci Eng C Mater Biol Appl. 2020;109:110538.
15. Choi JS, et al. Functional remodeling after vocal fold injury by small intestinal submucosa gel containing hepatocyte growth factor. Biomaterials. 2015;40:98–106.
16. Kim W, Kim GH. An intestinal model with a finger-like villus structure fabricated using a bioprinting process and collagen/SIS-based cell-laden bioink. Theranostics. 2020;10(6):2495–508.

17. Yang L, et al. Surface modified small intestinal submucosa membrane manipulates sequential immunomodulation coupled with enhanced angio- and osteogenesis towards ameliorative guided bone regeneration. Mater Sci Eng C Mater Biol Appl. 2021;119:111641.
18. Zhang XR, et al. Hypoxic preconditioning of human urine-derived stem cell-laden small intestinal submucosa enhances wound healing potential. Stem Cell Res Ther. 2020;11(1):150.
19. Zhang XZ, et al. Procyanidins-crosslinked small intestine submucosa: A bladder patch promotes smooth muscle regeneration and bladder function restoration in a rabbit model. Bioact Mater. 2021;6(6):1827–38.
20. Bi X, et al. The effects of silk layer-by-layer surface modification on the mechanical and structural retention of extracellular matrix scaffolds. Biomater Sci. 2020;8(14):4026–38.
21. Algarrahi K, et al. Acellular bi-layer silk fibroin scaffolds support functional tissue regeneration in a rat model of onlay esophagoplasty. Biomaterials. 2015;53:149–59.
22. Nagori CB, Panchal SY, Patel H. Endometrial regeneration using autologous adult stem cells followed by conception by in vitro fertilization in a patient of severe Asherman's syndrome. J Hum Reprod Sci. 2011;4(1):43–8.
23. Cao Y, et al. Allogeneic cell therapy using umbilical cord MSCs on collagen scaffolds for patients with recurrent uterine adhesion: a phase I clinical trial. Stem Cell Res Ther. 2018;9(1):192.
24. Phermthai T, et al. Successful derivation of xeno-free mesenchymal stem cell lines from endometrium of infertile women. Reprod Biol. 2016;16(4):261–8.
25. El Agha E, et al. Mesenchymal Stem Cells in Fibrotic Disease. Cell Stem Cell. 2017;21(2):166–77.
26. Eom YW, Shim KY, Baik SK. Mesenchymal stem cell therapy for liver fibrosis. Korean J Intern Med. 2015;30(5):580–9.
27. Ishiuchi N, et al. Hypoxia-preconditioned mesenchymal stem cells prevent renal fibrosis and inflammation in ischemia-reperfusion rats. Stem Cell Res Ther. 2020;11(1):130.
28. Shojaati G, et al. Mesenchymal Stem Cells Reduce Corneal Fibrosis and Inflammation via Extracellular Vesicle-Mediated Delivery of miRNA. Stem Cells Transl Med. 2019;8(11):1192–201.
29. Watanabe Y, et al. Mesenchymal Stem Cells and Induced Bone Marrow-Derived Macrophages Synergistically Improve Liver Fibrosis in Mice. Stem Cells Transl Med. 2019;8(3):271–84.
30. Han B, Chao J, Yao H. Circular RNA and its mechanisms in disease: From the bench to the clinic. Pharmacol Ther. 2018;187:31–44.
31. Salzman J. Circular RNA Expression: Its Potential Regulation and Function. Trends Genet. 2016;32(5):309–16.
32. Xu X, et al. CircRNA inhibits DNA damage repair by interacting with host gene. Mol Cancer. 2020;19(1):128.
33. Chen J, et al. circPTN sponges miR-145-5p/miR-330-5p to promote proliferation and stemness in glioma. J Exp Clin Cancer Res. 2019;38(1):398.

34. Yang H, et al. CircRNA BIRC6 promotes non-small cell lung cancer cell progression by sponging microRNA-145. Cell Oncol (Dordr). 2020;43(3):477–88.
35. Xu Q, et al. CircHIPK3 regulates pulmonary fibrosis by facilitating glycolysis in miR-30a-3p/FOXK2-dependent manner. Int J Biol Sci. 2021;17(9):2294–307.
36. Stella M, et al., *Serum Extracellular Vesicle-Derived circHIPK3 and circSMARCA5 Are Two Novel Diagnostic Biomarkers for Glioblastoma Multiforme*. Pharmaceuticals (Basel), 2021. 14(7).
37. Hsu YC, et al. Mitochondria in mesenchymal stem cell biology and cell therapy: From cellular differentiation to mitochondrial transfer. Semin Cell Dev Biol. 2016;52:119–31.
38. Li Q, et al. The role of mitochondria in osteogenic, adipogenic and chondrogenic differentiation of mesenchymal stem cells. Protein Cell. 2017;8(6):439–45.
39. Mahrouf-Yorgov M, et al. Mesenchymal stem cells sense mitochondria released from damaged cells as danger signals to activate their rescue properties. Cell Death Differ. 2017;24(7):1224–38.
40. Phinney DG, et al. Mesenchymal stem cells use extracellular vesicles to outsource mitophagy and shuttle microRNAs. Nat Commun. 2015;6:8472.
41. Wanet A, et al. Connecting Mitochondria, Metabolism, and Stem Cell Fate. Stem Cells Dev. 2015;24(17):1957–71.
42. Wang J, et al. Cell adhesion-mediated mitochondria transfer contributes to mesenchymal stem cell-induced chemoresistance on T cell acute lymphoblastic leukemia cells. J Hematol Oncol. 2018;11(1):11.
43. Chen J, et al. Mesenchymal stem cell-derived exosomes protect beta cells against hypoxia-induced apoptosis via miR-21 by alleviating ER stress and inhibiting p38 MAPK phosphorylation. Stem Cell Res Ther. 2020;11(1):97.
44. Wobma HM, et al. The influence of hypoxia and IFN-gamma on the proteome and metabolome of therapeutic mesenchymal stem cells. Biomaterials. 2018;167:226–34.

Figures

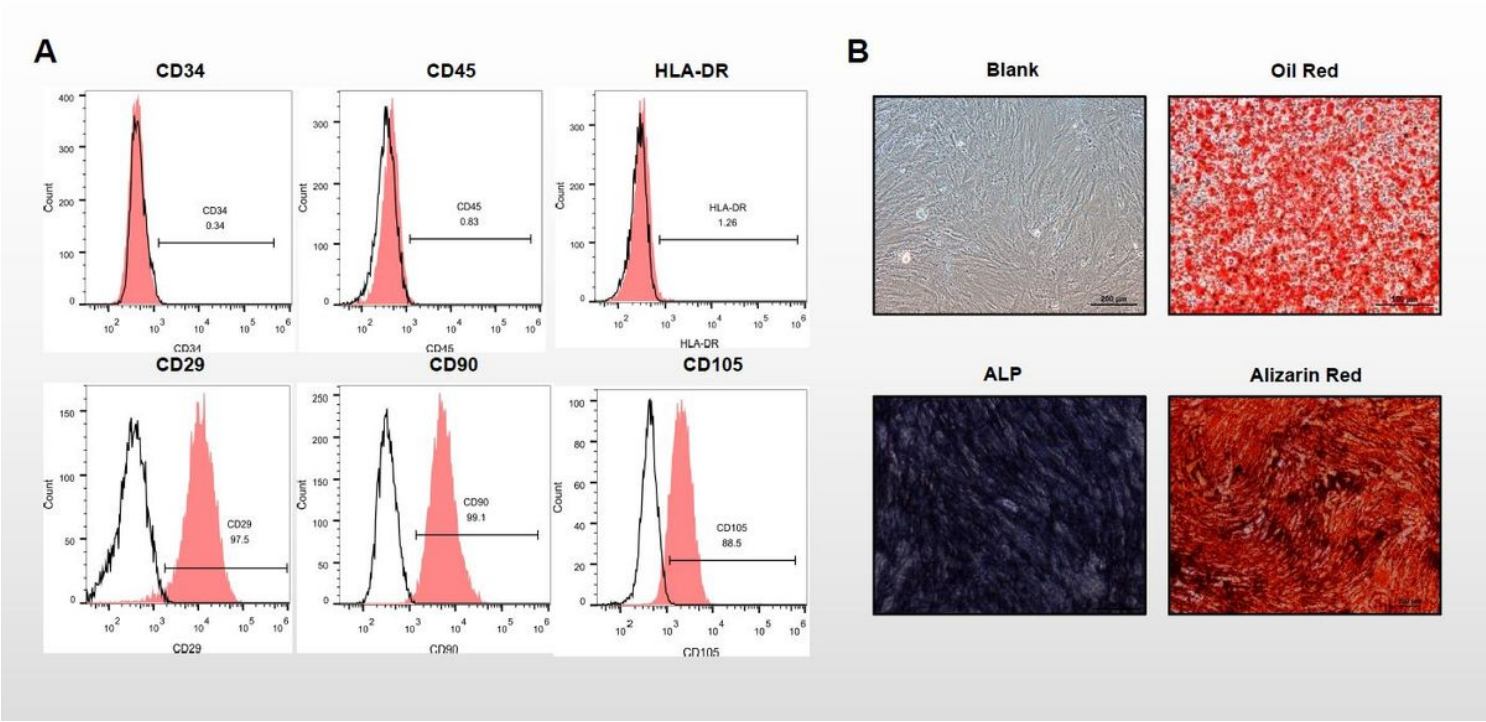

Figure 1

Culture and characterization of HuMSCs. (A) The cell morphology of the cultured HuMSCs. (B) The cell markers were analyzed by FACs. N=3.

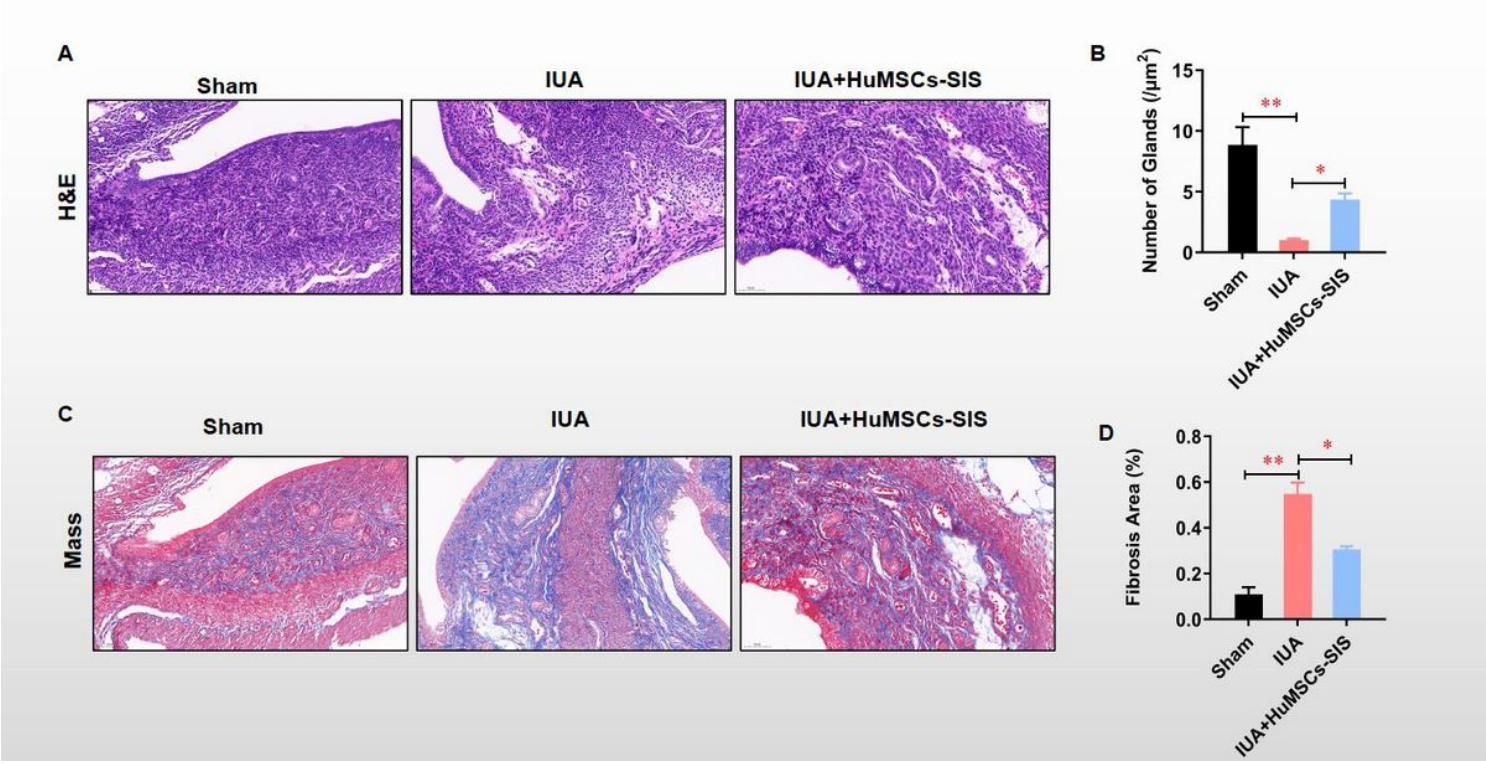

Figure 2

HuMSCs-SF-SIS increased the number of glands and reduced the area of fibrosis in the IUA model (A) The number of endometrial glands and the lumen of neonates were analyzed by HE staining. (B) Statistical analysis were performed to evaluate the number of endometrial glands. (C) The extent of fibrosis was assessed with Masson staining. (D) The fibrotic area of endometrium was carried out using Image J software. N=3. *P<0.05 indicated group.

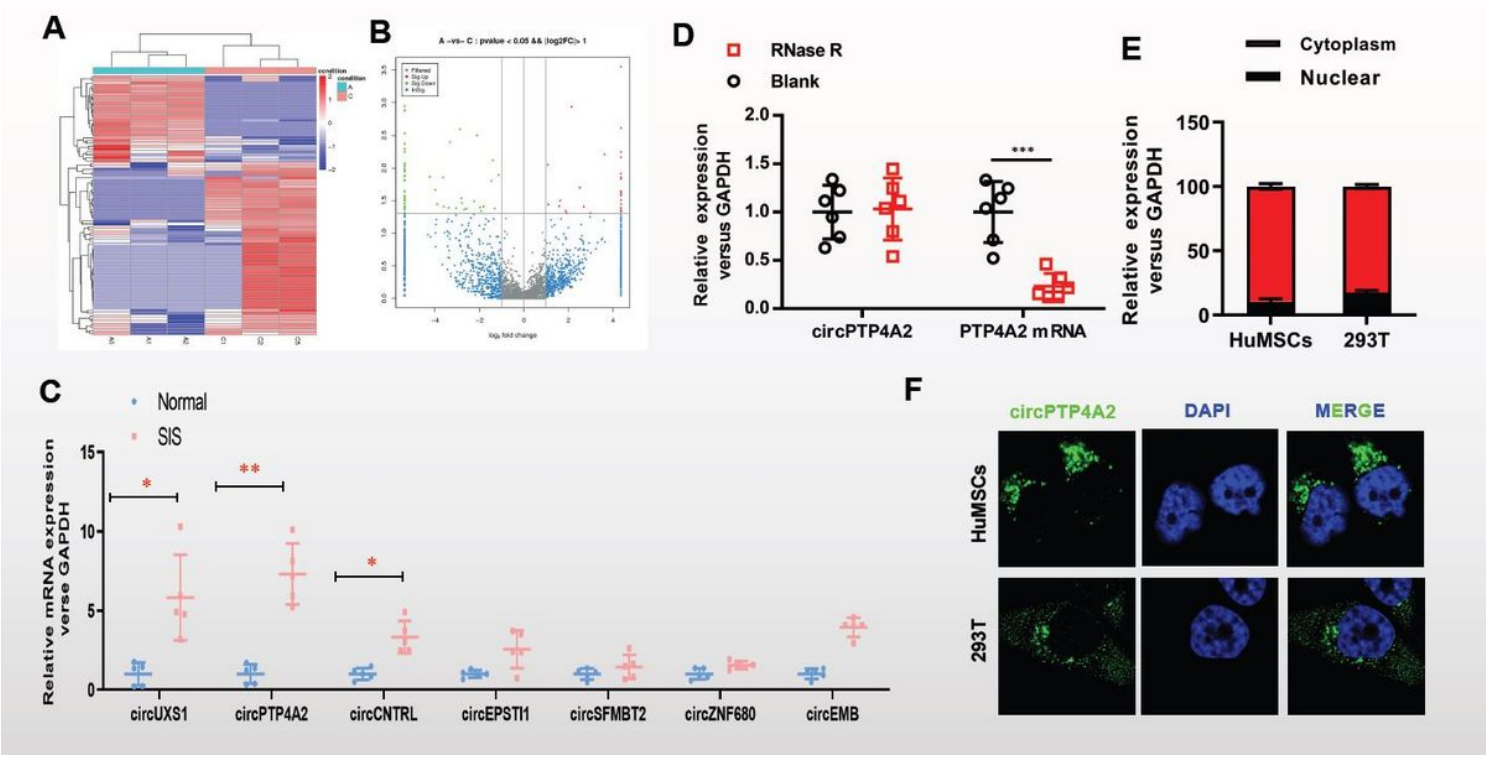

Figure 3

The expression level of circPTP4A2 is significantly elevated in the HuMSCs cultured on the SF-SIS scaffolds. (A)The profile of circRNA from normal HuMSCs and HuMSCs cultured on the SF-SIS scaffolds were analyzed by performing RNA-seq on ribosomal RNA-depleted total RNA. (B)The differential expression of total circRNAs was directly revealed by volcanic eruption-type clustering analysis. (C) Several significant up-regulated circRNAs (circUXSI , circPTP4A2, circCNTRL, circEPSTM, circSFMBT2, circZNF680 and circEMB) were verified via real-time PCR. (D) CircPTP4A2 was identified by real-time PCR, indicating a resistance between circPTP4A2 and RNase R.And the RNase R-treated PTP4A2 mRNA was significantly reduced. (E) Sub-fractional real-time PCR and (F) fluorescence in situ hybridization (FISH) assay was used to analyze the sub-cellular location of circPTP4A2 in HuMSCs. N=3, P< 0.05 indicated group.

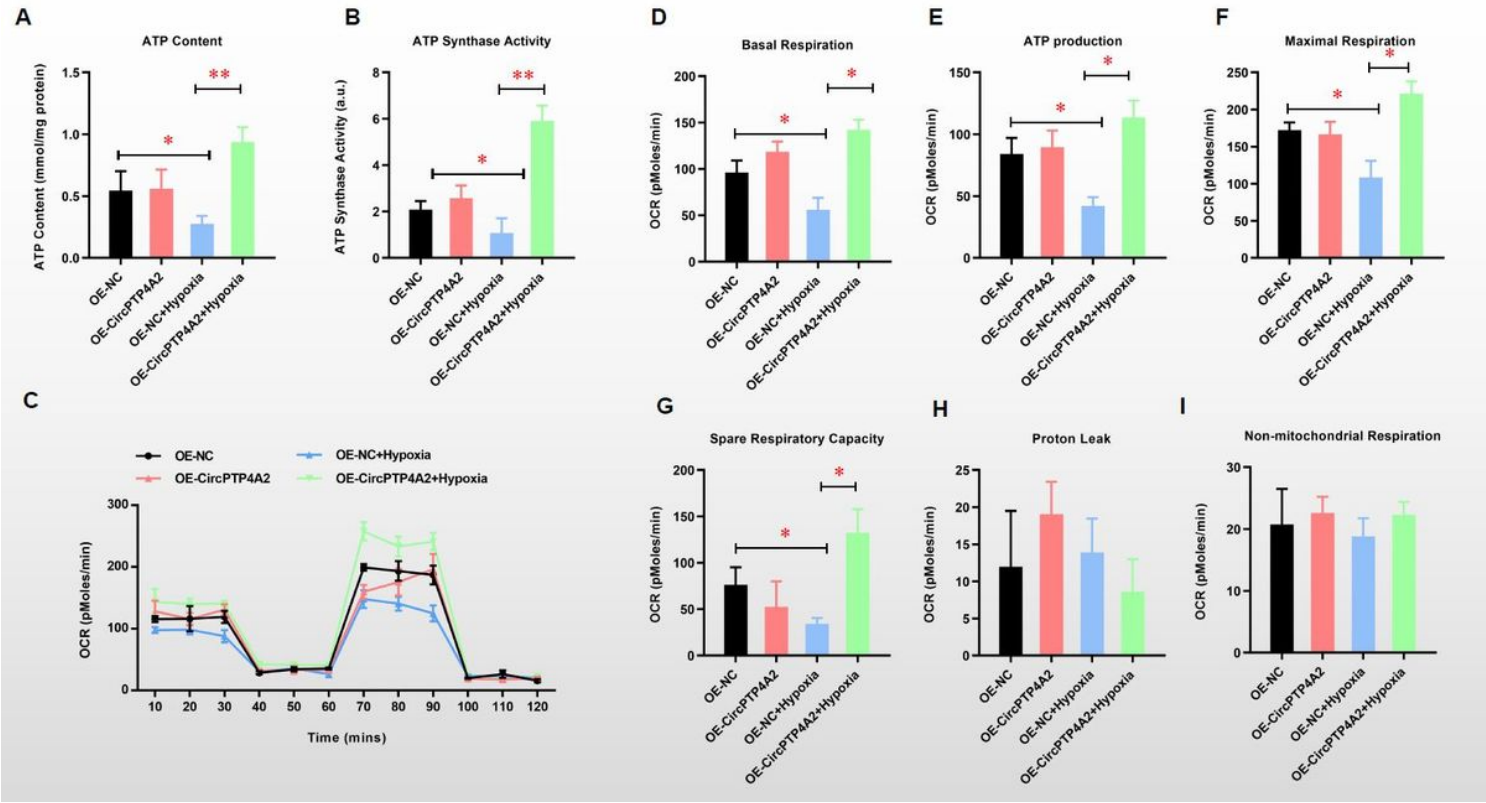

Figure 4

CircPTP4A2 facilitates the mitochondrial metabolism of HuMSCs under hypoxia condition. (A) The effects of circPTP4A2 on the ATP content and (B) ATP synthase activity was analyzed by kits. (C) The cell oxygen consumption rate (OCR) of HuMSCs was analyzed by the seahorse XF24 Extracellular Flux Analyser (D) The Basal Respiration, (E) ATP production (F) Maximal Respiration, (G) Spare Respiratory Capacity, (H)Proton leak and (I) non-mitochondrial Respiration were analyzed. N=3. *P< 0.05 indicated group.

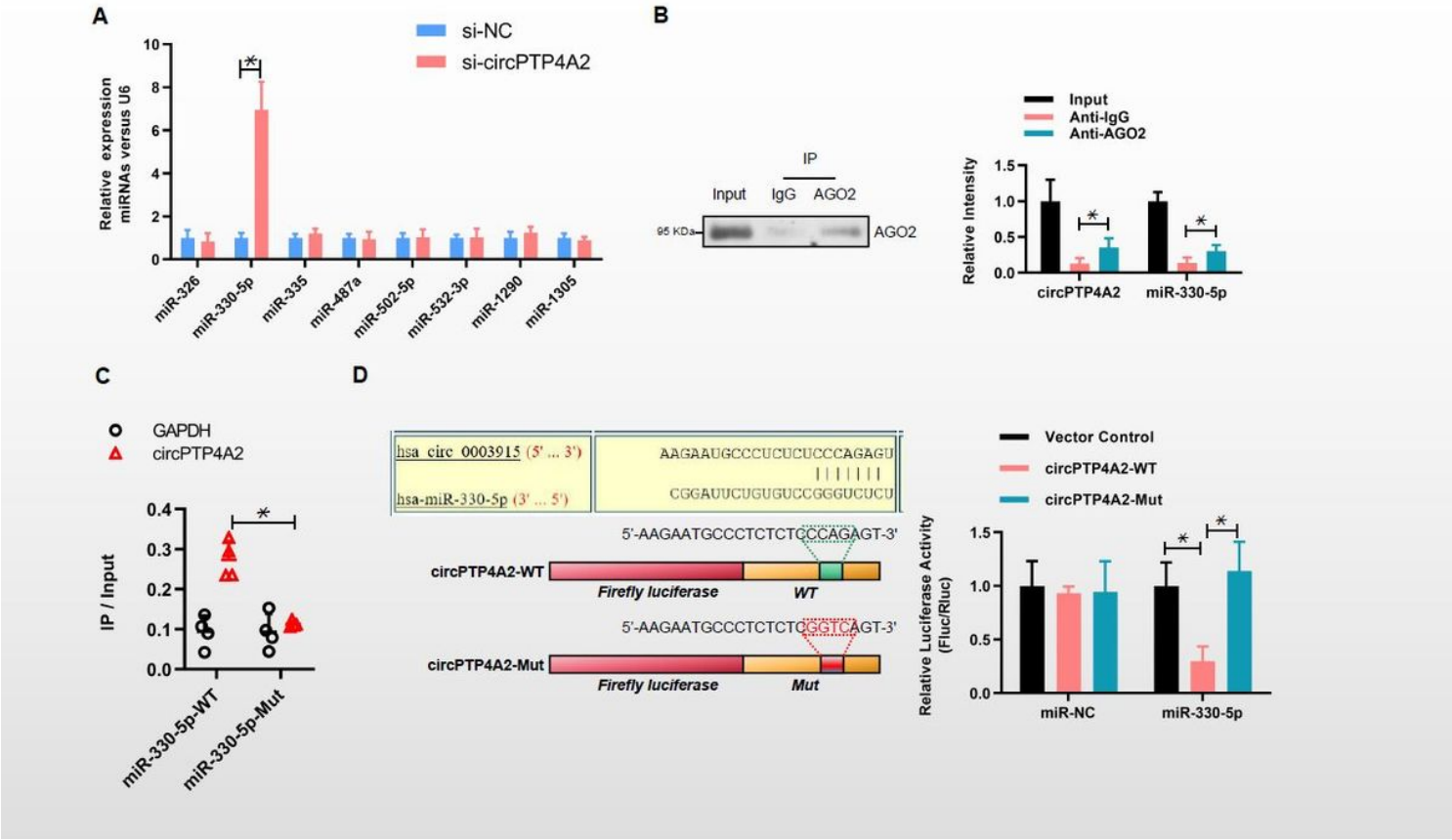

Figure 5

CircPTP4A2 is targeted by miR-330-5p in HuMSCs cells. (A) The level of miRNAs (miR-487a, miR-330-5p, miR-1290, miR-326,miR421, miR-502-5p, miR-532-3p, miR-335 and miR-1305) in HuMSCs cells with or without circPTP4A2 knockout were analyzed by real-time PCR. (B) Ago2 Co-Immunoprecipitation assay and (C) miR-330-5p RNA pull down were used to evaluate the interaction between miR-330-5p and circPTP4A2. (D) Dual-luciferase reporter assay was used to evaluate the control of miR-30-5p on circPTP4A2 in HuMSCs cells. N=3. *P< 0.05 indicated group.

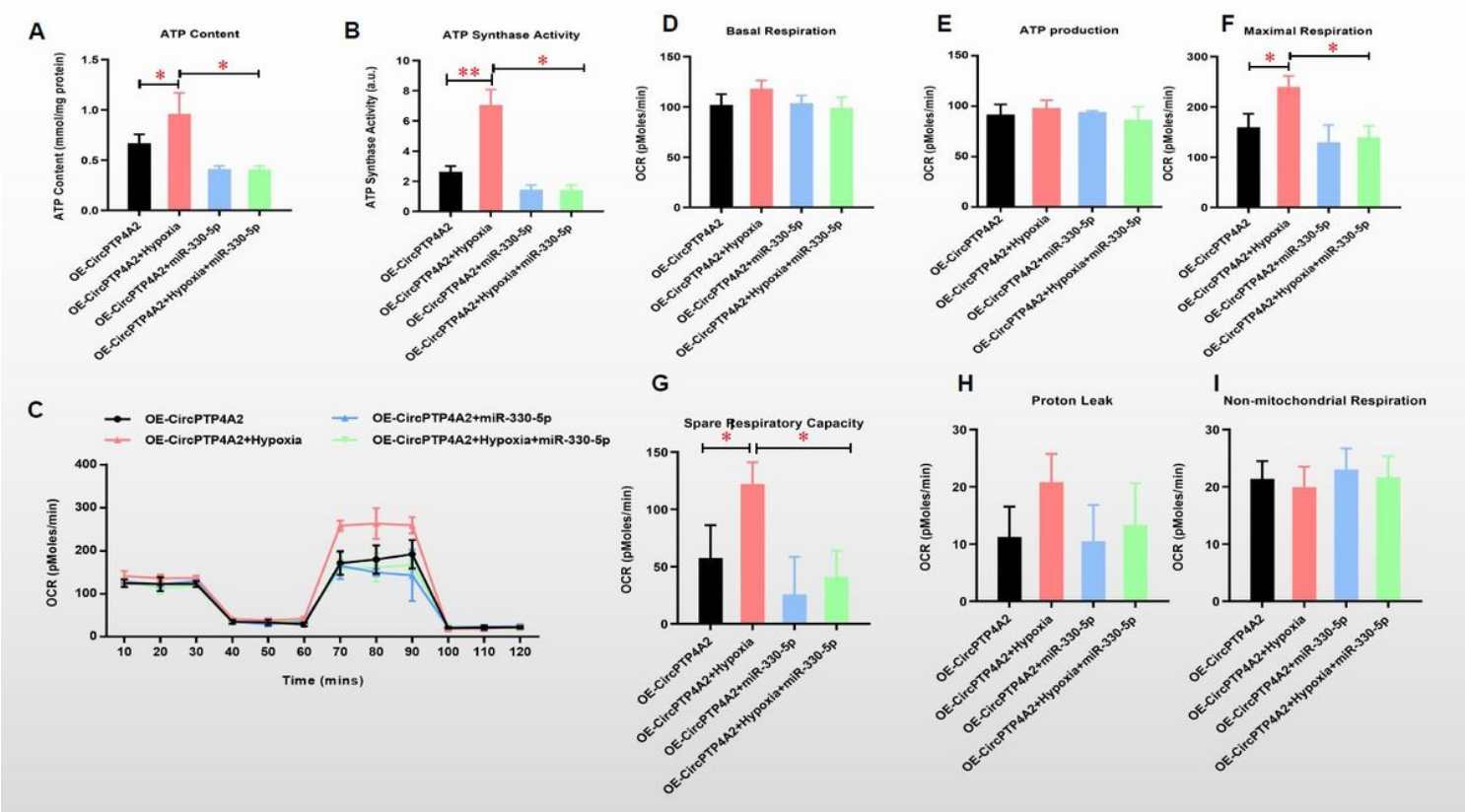

Figure 6

MiR-330-5p overexpression impairs the circPTP4A2 enhanced mit ochondrial metabolism in hypoxia treated HuMSCs. (A) The rescuer effects of miR-330-5p on the circPTP4A2 enhanced ATP content and (B) ATP synthase activity was analyzed by kits. (C) The rescuer effects of miR-330-5p on the circPTP4A2 enhanced cell oxygen consumption rate (OCR) of HuMSCs was analyzed by the seahorse XF24 Extracellular Flux Analyser. (D) The Basal Respiration, (E) ATP production (F) Maximal Respiration, (G) Spare Respiratory Capacity, (H) Proton leak and (I) non-mitochondrial Respiration were analyzed. N=3. *P< 0.05 indicated group.

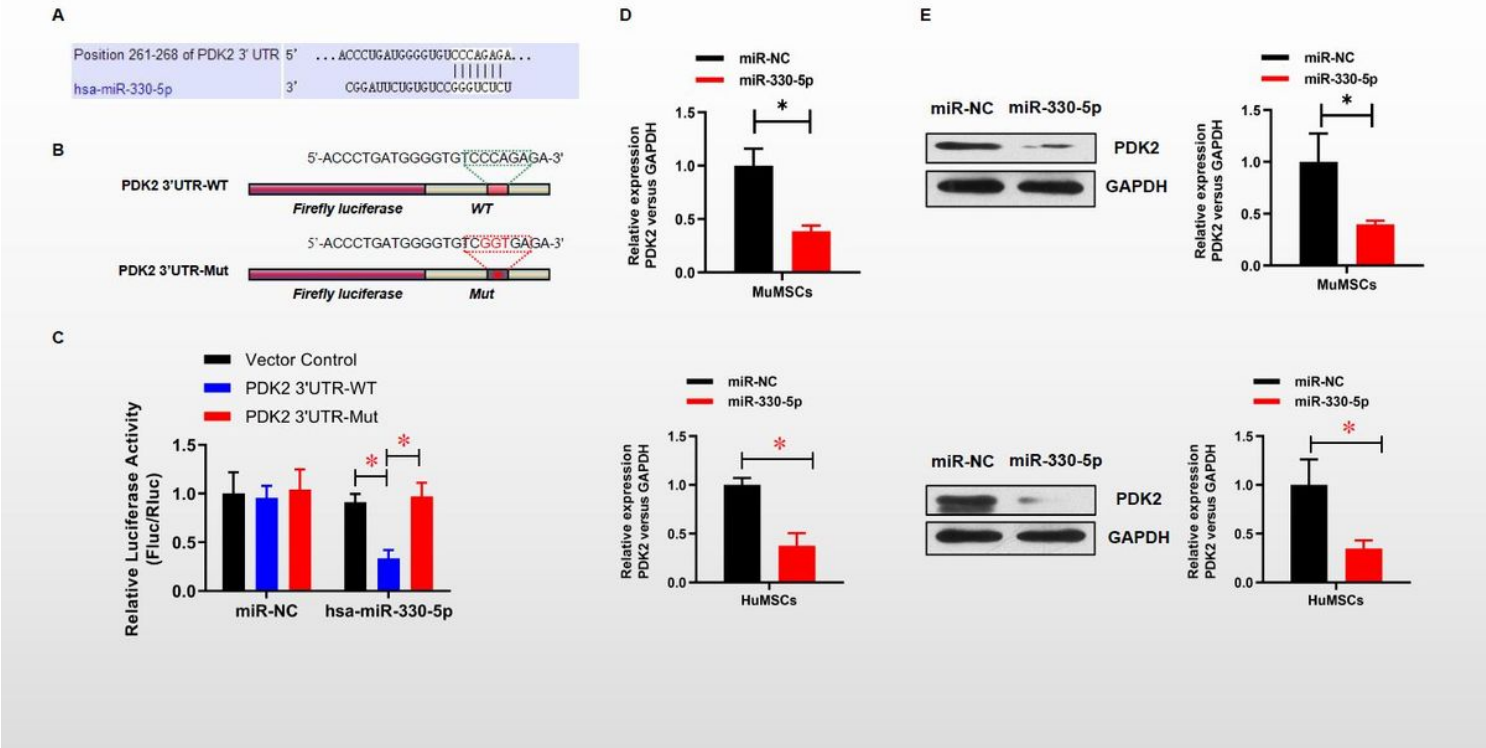

Figure 7

MiR-330-5p suppresses the expression of PDK2 via the 3'UTR target region. (A-C) Dual-luciferase reporter assay was used to evaluate the control of miR-30-5p on PDK2 mRNA 3'UTR in HuMSCs cells. (D)The mRNA and (E) protein levels of PDK2 in mouse umbilical MSCs and HuMSCs was analyzed by real-time PCR and Western Blot. N=3. *P<0.05 indicated group.

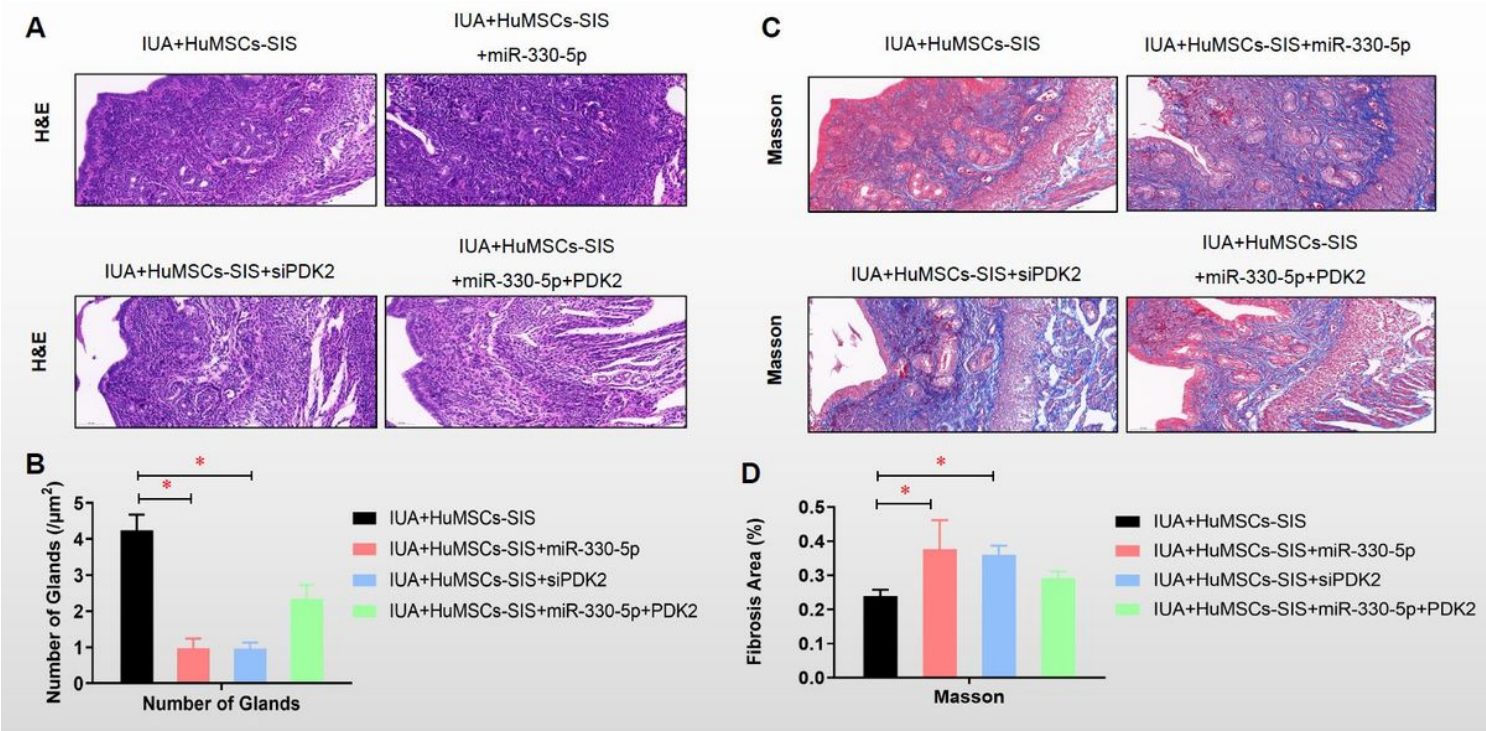

Figure 8

CircPTP4A2-miR-330-5p-PDK2 signaling is critical to the HuMSCs-SF-SIS increased number of glands and decreased fibrosis area in IUA model. (A) The number of endometrial glands and the lumen of neonates was analyzed by HE staining. (B) Statistical analysis was performed to evaluate the number of endometrial glands. (C) The degree of fibrosis was assessed using Masson staining. (D) The fibrotic area of endometrium was carried out using Image J software. N=3. *P< 0.05 indicated group.